ISSN: 1410-8917
e-ISSN: 2597-9914

Jurnal Kimia Sains dan Aplikasi 26 (10) (2023): 381-390

Jurnal Kimia Sains dan Aplikasi
Journal of Scientific and Applied Chemistry

Journal homepage: http://ejournal.undip.ac.id/index.php/ksa

Fabrication and Characterization of Chitosan-Polyvinyl Pyrolidone K-30 for Creatinine Transport Membranes

Retno Ariadi Lusiana [1,*], Riska Nurfida Annisa [1], Vinsencius Guntur Pandu Marcellino [1], Didik Setiyo Widodo [1], Hasan Muhtar [1]

[1] Department of Chemistry, Faculty of Science and Mathematics, Diponegoro University, Semarang 50275, Indonesia

* Corresponding author: retno.lusiana@live.undip.ac.id

https://doi.org/10.14710/jksa.26.10.381-390

Article Info

Article history:

Received: 11th November 2023
Revised: 29th November 2023
Accepted: 01st December 2023
Online: 23rd December 2023

Keywords:
Hydrophilicity; Chitosan; Creatinine; Membrane; PVP; Transport

Abstract

The investigation of membrane-based hemodialysis is an interesting study due to its efficacy in eliminating metabolic waste compounds, such as creatinine, from the body. However, not all membrane types exhibit optimal transport capabilities, necessitating modifications. In this study, we conducted modifications on chitosan (CS) membranes by incorporating polyvinyl pyrrolidone K-30 (PVP K-30) and assessing their physicochemical characteristics. The modified membrane underwent characterization and subsequent evaluation of its transport capabilities. The primary objective of this research is to design a membrane composed of chitosan and PVP K-30 with enhanced creatinine transport capabilities. The study commenced with the fabrication of CS membranes combined with CS-PVP, involving six variations of CS and PVP K-30 with volume ratios of 5:0, 4:1, 3:2, 1:1, 2:3, and 4:1. The resulting solution was then printed into a flat sheet membrane. All completed membranes underwent comprehensive characterization, including tests for functional groups using Fourier Transform Infrared (FTIR), membrane weight and thickness, porosity, water absorption, swelling, hydrophilicity, pH resistance, and biodegradation. In the final phase, the membrane was utilized in the creatinine transport process. FTIR analysis of the CS-PVP K-30 membrane revealed O-H and N-H group spectra at wave numbers 3363.06 cm^{-1} and 1587.17 cm^{-1}, indicating hydrogen bonding between the two polymers. Characterization tests demonstrated that the CS-PVP membrane exhibited increased porosity, water absorption, swelling, and hydrophilicity. In the creatinine transport test, the CS-PVP membrane demonstrated enhanced creatinine transport ability compared to the CS membrane. The highest clearance value for creatinine was observed in the CS-PVP5 membrane, with an increase in the amount of PVP K-30 correlating with an elevated creatinine clearance value. The creatinine clearance values for the CS membrane, CS-PVP1, CS-PVP2, CS-PVP3, CS-PVP4, and CS-PVP5 were 0.30, 0.36, 0.37, 0.39, 0.42, and 0.46 mg/dL, respectively.

1. Introduction

The membrane is a thin, selective, and semipermeable layer located between two phases. These phases consist of the source phase, harboring trapped components, and the acceptor phase, housing components capable of permeating the membrane [1]. The field of membrane technology is experiencing rapid growth with continuous refinement of methods. Components and material structures within membranes play pivotal roles in advancing membrane-based technology. The utilization of membrane technology has expanded across various sectors, encompassing food and beverages, water treatment, industrial waste processing, and the medical field. One application of membrane technology in the medical industry is hemodialysis via dialyzer membranes [2].

Hemodialysis is a biomedical procedure that replaces kidney function by eliminating metabolic waste

substances from the body, specifically creatinine, urea, and glucose. The normal range for serum creatinine is 0.7 - 1.3 mg/dL in men and 0.6 - 1.1 mg/dL in women; elevated creatinine levels indicate potential kidney disease [3]. The fundamental principle of hemodialysis relies on diffusing toxic uremic compounds from the body into the dialysate solution through a semipermeable membrane driven by concentration or pressure differentials [4]. When employing membranes for hemodialysis, specific essential characteristics must be present. These include small, uniformly distributed pores, hemocompatibility, mechanical robustness, leak resistance, selectivity, active groups facilitating permeate capture through hydrogen bond formation, and reactivity [5].

The primary materials for membranes can be derived from natural and synthetic polymers. Natural polymers possess distinctive attributes, including degradability, biocompatibility, non-toxicity, and ease of regeneration. Chitosan (CS) is a notable natural polymer with membrane potential, derived as a polyaminosaccharide from the deacetylation of chitin in an alkaline environment. Remarkably, it ranks as the second-largest raw material reserve in nature [6]. CS serves as an inert biopolymer suitable for application as a hemodialysis membrane. However, its functional groups exhibit insufficient reactivity for effective interaction with target compounds [7, 8]. While CS is hydrophobic in water, the amine group on the CS backbone ($-NH_2$) becomes protonized in acidic conditions, rendering the material positively charged. The positive charge of the primary amine group on the CS membrane enables protein adsorption to the membrane surface, driven by electrostatic forces between the positive charge and the negative charge on the protein. Unfortunately, this phenomenon diminishes membrane permeability and triggers blood clotting [9].

Regarding the manufacturing process, producing CS membranes is comparatively simpler and requires less time when juxtaposed with the fabrication of synthetic membranes [10]. Nevertheless, membranes crafted solely from CS exhibit several drawbacks, encompassing diminished porosity, low stability, a deficiency in active sites, and limited hydrophilicity. Consequently, when utilized for dialysis, the outcomes remain suboptimal [11]. Modifying the CS membrane becomes imperative to address these shortcomings in structure and surface properties. Three viable approaches for modifying CS are through cross-linking reactions, grafting reactions, and alloying [1].

Polyvinyl pyrrolidone (PVP), a synthetic polymer, exhibits commendable biocompatibility and has, over the years, found application as a biomaterial or additive in pharmaceutical compositions [12]. Widely recognized, PVP serves as a popular polymer additive in the production of ultrafiltration (UF) or nanofiltration (NF) membranes [13]. Its application as an additive in hemodialysis proves advantageous, where its presence in the PES/PVP mixture enhances hydrophilicity, pore size (leading to heightened flux rates), antifouling properties, resistance to proteins, and the membrane's ability to clear uremic solutes (urea, creatinine) [14]. Combining natural and synthetic polymers results in novel materials boasting enhanced mechanical properties and reduced costs. The blending of CS and PVP induces the formation of hydrogen bonds between CS and PVP molecules, facilitated by the amino and hydroxyl groups in CS and the C=O groups in PVP, culminating in a material with distinct characteristics [15].

The synthesis and characterization of CS/PVP biocomposites for biomedical applications is a subject of investigation. A robust interaction between CS and PVP is observed, facilitated by the formation of hydrogen bonds, as confirmed by ATR-FTIR. Incorporating PVP leads to an enhancement in the tensile strength and swelling degree of the CS/PVP mixed membrane [16]. A mucoadhesive membrane comprising CS and PVP has been developed as a drug delivery system. The presence of PVP in the membrane fosters a chemical interaction with CS, resulting in increased thermal stability, heightened membrane swelling ratio, and enhanced mucoadhesion [17]. Examination through SEM indicates well-distributed components in the biocomposite containing CS, PVA, and PVP, signifying that PVA and PVP macromolecules are embedded in the CS matrix due to robust interactions. This biocomposite demonstrates effective antibacterial activity against Escherichia coli and Staphylococcus aureus, suggesting its potential as a wound dressing material [18]. In the research focused on CS/PVP mixed membranes, cross-linking assisted by UV (ultraviolet) radiation is employed. The resulting membrane exhibits a smooth surface, and UV-assisted cross-linked CS/PVP blend membranes demonstrate excellent performance in the pervaporation separation of methanol/ethylene glycol (EG) and water/ethanol. The degree of swelling increases with the addition of PVP [19].

Building upon findings from multiple previous studies, CS has been blended with PVP to enhance hydrophilicity and biocompatibility, resulting in the development of a reactive membrane. This combination of CS and PVP has previously found applications in drug delivery systems, wound dressings, and pervaporation separation. Building on the research demonstrating CS's potential as a dialysis membrane, researchers aim to create a CS membrane blended with PVP specifically for creatinine transport applications. PVP was selected as an additive in CS membrane alloys due to its suitability for hemodialysis, contributing to increased hydrophilicity, biocompatibility, enlarged pores, and enhanced permeation ability.

The presence of PVP induces hydrophilic N-H groups, intensifying the membrane's interaction with water. The anticipated outcome is an elevation in permeation ability through enhanced hydrogen bond formation between the two polymers. This effort aims to enhance the characteristics of CS membranes, gearing them for improved performance in creatinine transport applications. Vitamin B12, commonly present in blood, is also considered and evaluated in the assessment of membrane activity for hemodialysis. Testing for vitamin B12 serves as a comparative measure for membrane selectivity, especially in comparison to compounds larger than creatinine.

2. Experimental

2.1. Materials and Tools

Chitosan (BM = 40,000 g/mol) (chimultiguna Lab, Cirebon, Indonesia, DD: 87%), Acetic acid p.a (Merck), Polyvinyl pyrrolidone (PVP K-30) (chimultiguna Lab, Cirebon, Indonesia, purity >90%), distilled water, NaOH (BM = 40 g/mol) (Merck), Creatinine (BM = 113.11 g/mol) (Merck), Picric acid (BM = 229.11 g/mol) (Merck), and Vitamin B12 (Supra Ferbindo Farma).

Membrane functional groups were determined using an FT-IR spectrophotometer (Perkin Elmer, USA). The transport sample concentration was measured with a Thermo Scientific TM GENESYS 10S UV-Visible spectrophotometer (Waltham, MA, USA) and pH meter (Hanna series HI9024, USA).

2.2. Preparation of Membrane

Membrane manufacturing was based on a phase inversion process, employing a composition of materials outlined in Table 1. The reaction was conducted at a temperature of 50-60°C, with a stirring time of 2 hours. In the initial phase, a 1.5% chitosan (CS) solution in 1% acetic acid and a 1.5% polyvinyl pyrrolidone (PVP) solution in warm water were prepared. After preparing all solutions, they were mixed and stirred for 2 hours according to the composition specified in Table 1. The solution mixture was subjected to ultrasonication at 55°C for 15 minutes to complete the reaction. Subsequently, the mixture was cooled and molded into a flat sheet by pouring the solution into a petri dish, then drying in an oven at 35°C for 12 hours until it reached a dry state. The resulting dry membrane underwent treatment with NaOH to detach it from the petri dish. The membrane was washed with water until achieving a neutral pH and dried [1].

2.3. Functional Group Analysis Using FTIR

Membrane functional group analysis was performed using an FT-IR spectrophotometer (Perkin Elmer). A thin membrane sheet was placed in the sample holder and measured at a wavenumber of 500-4000 cm^{-1}.

2.4. Membrane Porosity Measurement

Determining membrane porosity involved immersing a 15 × 3 cm-sized membrane in 10 mL of distilled water for 24 hours. Subsequently, the water on the membrane's surface was removed using a tissue, and the initial wet weight of the membrane was measured. Following this, the membrane was dried in an oven set at 100°C for 6 hours. After cooling, the membrane was weighed again to determine its dry weight. The percentage of membrane porosity was then calculated using the formula presented in Equation (1).

$$\text{Porosity (\%)} = \frac{(Ww-Wd)}{(\rho w.V)} \text{x100} \quad (1)$$

where, the wet weight (Ww) and dry weight (Wd) were denoted as weights in grams. The density of water (ρw) was established as 1 $g.cm^{-3}$, and V represented the volume of the membrane in cubic centimeters (cm^3). Weight measurements were conducted thrice to assess the reliability and consistency of the measurements.

2.5. Hydrophilicity of Membrane

The membrane hydrophilicity was quantified by employing the sessile drop method, a technique characterizing the membrane's capacity to absorb water deposited onto its surface. A water contact angle, indicative of the angle formed between the water droplet and the membrane, was employed for assessment. A diminished contact angle value signified the hydrophilic nature of the membrane. Photographic documentation of water droplets and subsequent contact angle measurements were conducted using ImageJ software. To ensure reliability, the contact angle measurements were performed three times, thereby validating the consistency of the results [20].

2.6. Water Uptake (WU) and Swelling Degree (SD)

The assessment of water absorption stands as a crucial determinant of membrane properties, offering insights into both hydrophilicity and hydrophobicity, thereby reflecting the extent of membrane expansion. To ascertain the WU, a membrane measuring 15×3 cm underwent a soaking process in water for 6 hours, with weight measurements conducted before and after immersion. Similarly, the SD was determined by immersing the membrane in water for 24 hours, followed by measuring the membrane diameter before and after the immersion period. The percentage values for WU and SD were then computed using Equations (2) and (3), respectively. In these equations, Wt denotes the weight of the membrane after soaking (in grams), Wo signifies the weight of the membrane before soaking (in grams), and Io and It represent the membrane diameter before and after immersion (in centimeters), respectively. In order to ensure the reliability and consistency of the measurements, the weight measurements were repeated three times.

$$\text{WU} = \frac{Wt-Wo}{Wo} \times 100 \quad (2)$$

$$\text{SD} = \frac{\text{It}}{\text{Io}} \times 100 \quad (3)$$

Table 1. Composition ratio of membrane

Membrane	Ratio	Volume of CS (mL)	Volume of PVP K-30 (mL)
CS	5:0	5	0
CS-PVP1	4:1	4	1
CS-PVP2	3:2	3	2
CS-PVP3	1:1	2.5	2.5
CS-PVP4	2:3	2	3
CS-PVP5	1:4	1	4

2.7. Resistance to pH

Membrane samples, each sized 15×3 cm, were subjected to obtain the initial dry weight. Subsequently, these samples were immersed in 10 mL solutions with varying pH levels (3, 5, 7, 9, and 11) for 24 hours. The pH of the solution was adjusted using acetic acid and sodium hydroxide. Following the immersion, the membranes underwent a drying process, and their weights were measured again to determine the final dry weight. The pH resistance was quantified based on the weight loss incurred by the membrane, as per the calculation outlined in Equation (4).

$$W(\%) = \frac{Wo-Wt}{Wt} x\ 100 \quad (4)$$

where, Wo represents the initial membrane weight before immersion (in grams) and Wt denotes the final membrane weight after immersion (in grams). To ensure the reliability and consistency of the measurements, the weight assessments were conducted three times.

2.8. Membrane Biodegradation Test

In the biodegradation test, membrane evaluation involved planting all membrane samples in compost for 15 weeks. Before implantation, the initial weights of all membrane samples were recorded. The membranes were introduced into the compost and maintained under moist conditions with regular watering every week after the initial measurements. The assessment of biodegradation was conducted by quantifying the reduction in mass experienced by the membrane, as per the calculation presented in Equation (5).

$$W(\%) = \frac{Wo-Wi}{Wo} x\ 100 \quad (5)$$

where, Wo denotes the initial membrane weight before implantation (in grams), and Wi represents the membrane weight in weekly measurements (in grams). Weight assessments were conducted three times to ensure the reliability and consistency of the measurements [21].

2.9. Membrane Transport Assay

Membrane permeability, an indicator of the membrane's ability to transport creatinine, was assessed through a permeation test conducted with specialized tools. The membrane, featuring a diameter of 2.5 cm, was positioned at the center to segregate the source and acceptor components. The source was filled with a 1.5 mg/dL creatinine solution in 50 mL of phosphate buffer media, while the acceptor contained 50 mL of phosphate buffer. The transport process occurred over 6 hours at room temperature, with 2 mL samples extracted from the source and acceptor phases every hour. These samples underwent complexation with picric acid, and their absorbance was measured at 486 nm using a UV-Visible spectrophotometer. Membrane permeability to solutes, also known as clearance, was determined through Equation (6), wherein [S]o represents the source concentration at hour zero (mg/dL), and [S]t signifies the source concentration at a specific time (mg/dL).

$$Clearance = [S]o - [S]t \quad (6)$$

Additionally, a permeation test for vitamin B12 was conducted to evaluate membrane selectivity. This involved comparing the clearance values for creatinine and vitamin B12. The source phase was filled with 50 mL of a 1.5 mg/dL vitamin B12 solution in a phosphate buffer, while the acceptor phase contained a phosphate buffer solution. Vitamin B12 transport was conducted over 6 hours at room temperature, with samples extracted from both the source and acceptor phases every hour. The absorbance of these samples was measured using a UV-Vis spectrophotometer at a wavelength of 361 nm [22].

3. Results and Discussion

3.1. Membrane Characteristics

3.1.1. Functional Group Analysis

The CS spectrum in Figure 1 illustrates a broad band at 3361.15 cm^{-1}, indicative of O-H stretching. The band at 1587.32 cm^{-1} corresponds to N-H (amide II) (NH_2) bending, and a minor peak at 1645.91 cm^{-1} is attributed to C=O (amide I) O=C-NHR stretching [20]. The band at 2920.20 cm^{-1} represents the C-Hsp³ stretching vibration region, and the wavenumber 1323.89 cm^{-1} signifies the aromatic ring in the fingerprint region [23]. The peak at 1057.64 cm^{-1} indicates the stretching vibration of the C-O cyclic ether of CS [24]. In the PVP K-30 spectrum in Figure 1, 1648.34 cm^{-1} is linked to the C=O stretching absorption band, and the C-N peak is observed at the wavenumber 1283.61 cm^{-1} [25]. Absorption at wavenumbers 1492.92 cm^{-1} and 1459.87 cm^{-1} indicates the presence of C=C ring strain [26].

The interaction between CS and PVP K-30 is robust, resulting in the formation of a homogeneous phase due to strong hydrogen bonds. In Figure 1, the sharp peak at 1320.75 cm^{-1} in the CS-PVP spectrum corresponds to the C-N stretching vibration attributed to the pyrrolidone structure. The presence of peaks at 1587.17 cm^{-1} and 1320.75 cm^{-1} in the CS-PVP mixture confirms the homogeneous mixing between CS and PVP [27]. The peak position at 3363.09 cm^{-1} in CS shifted to a lower frequency in the CS-PVP mixture, confirming the interaction of CS and PVP through intermolecular hydrogen bonds. Additionally, the shift of the carbonyl bond from 1647.69 cm^{-1} to a lower frequency further validates the interaction between CS and PVP K-30. The functional group data obtained aligns with the literature findings of Kumar *et al.* [28].

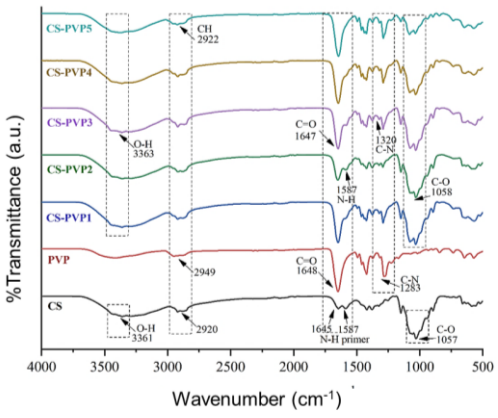

Figure 1. FTIR spectra of CS-PVP membranes

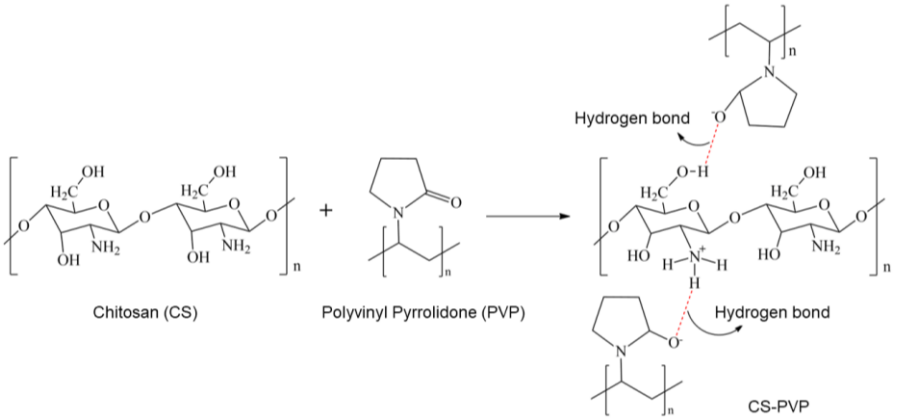

Figure 2. Proposed interaction between CS and PVP

CS, acting as a hydrogen donor, forms hydrogen bonds with the carbonyl group of PVP K-30. The pyrrolidone ring in PVP K-30 contains a proton that accepts a carbonyl moiety, while CS presents hydroxyl and amino groups as side groups. Consequently, hydrogen bonding interactions are likely to occur between these two chemical moieties in the mixture of CS and PVP K-30. Figure 2 visually represents the estimated interaction between CS and PVP K-30.

3.1.2. Membrane Porosity

The modification of CS with PVP has notable effects on the weight, thickness, and porosity of the resulting membrane. The mass content of the membrane, as detailed in Table 2, signifies variations in weight and thickness. The observed differences in membrane thickness align with changes in the alloy composition. Specifically, increased mass content corresponds to higher membrane weight and thickness [20]. As CS serves as the primary constituent of the membrane and PVP K- 30 acts as an additive, a higher CS content results in a denser membrane.

Table 2 reveals that membrane compositions with elevated amounts of PVP K-30 exhibit greater porosity values. This phenomenon arises from PVP K-30 acting as an additive capable of enhancing membrane porosity. The addition of PVP to the casting solution leads to increased porosity, facilitated by the diffusion of additives at low concentrations, thereby forming larger pores [29]. In this context, PVP functions as a pore former during membrane formation, and the capacity for pore formation increases with higher PVP content in the membrane [30].

3.1.3. Membrane Hydrophilicity

Table 2 presents the contact angle data, indicating that the incorporation of PVP K-30 into the CS membrane results in a reduction of the membrane contact angle. This reduction signifies an enhancement in the hydrophilicity of the membrane. The introduction of PVP K-30 contributes to increased hydrophilicity by leveraging the effect of N-H hydrophilic groups, thereby fostering heightened interaction between the membrane and water. During the phase inversion process, hydrophilic additives migrate to the water interface with the polymer, leading to a greater density of hydrophilic hydroxyl groups on the surface and, consequently, increased hydrophilicity [31].

3.1.4. Water Uptake (WU) and Swelling Degree (SD)

The membrane's water absorption capacity is determined by the number of vacant cavities and the interaction ability of the molecules composing the membrane with diffusing water molecules. The data presented in Table 2 reveals that an augmentation in water uptake is observed in membranes with higher concentrations of PVP K-30, while membranes with increased CS content tend to exhibit lower water uptake. The elevated percentage of water absorption in the membrane is attributed to the addition of PVP K-30, characterized by hydrophilic -OH groups. This addition increases the overall hydrophilicity of the membrane, consequently enhancing its water absorption capacity. A strategic approach to boost water absorption involves blending the polymer with a highly hydrophilic counterpart, such as PVP [32].

The membrane's pronounced swelling properties stem from the inherently hydrophilic nature of the material [16]. The swelling outcomes for the membrane are detailed in Table 2. PVP, being hydrophilic, engages in physical interactions with water molecules through intermolecular hydrogen bonding, thereby amplifying the membrane's hydrophilicity. The heightened hydrophilicity facilitates water ingress into the membrane's cavities, leading to an increased swelling value. The volume expansion of the membrane accelerates notably as the PVP content in the membrane rises [33]. The heightened PVP K-30 content in the membrane compound mixture augments the overall volume and interactions between spaces, particularly through hydrogen bonding, resulting in amplified water absorption.

Table 2. Physicochemical properties of membranes

Membranes	Weight (mg)	Thickness (µm)	Porosity (%)	Swelling Degree (%)	Water Uptake (%)	Water Contact Angle (°)
CS	74.98±0.76	7.62±0.16	62.62±1.27	131.09±1.78	49.47±0.98	78.38±1.07
CS-PVP1	70.48±0.67	7.50±0.23	73.09±1.13	134.46±1.82	61.67±1.16	65.66±0.96
CS-PVP2	57.94±0.89	7.30±0.13	101.36±1.21	135.03±1.89	68.05±1.21	57.26±1.16
CS-PVP3	53.66±0.73	7.10±0.18	170.24±1.21	138.56±1.65	76.78±1.18	49.22±1.13
CS-PVP4	48.54±0.65	6.70±0.21	172.92±1.23	144.90±1.72	104.38±1.17	45.34±1.12
CS-PVP5	42.44±0.84	5.94±0.26	265.04±1.31	148.37±1.69	208.55±1.24	43.92±1.21

3.2. Membrane Stability

3.2.1. Resistance to pH

The purpose of subjecting the membrane to resistance testing under various pH conditions is to evaluate its stability across a spectrum of pH environments. In Figure 3, the most substantial weight loss for the membrane was observed at pH 3, a trend observed across all membrane types. This phenomenon indicates that pH 3 represents conditions capable of decomposing both CS and the components of CS combined with PVP K-30. Under highly acidic pH conditions, CS tends to re-dissolve in an acidic environment [34]. At pH 7, there is no discernible decrease in membrane weight, signifying that the membrane remains normal or stable. However, under alkaline conditions (pH 9 and pH 11), a reduction in membrane weight occurs. This is attributed to the ingress of NaOH into the membrane, contributing negative ions to the membrane's functional groups, leading to the transformation of the -NH_2 group to an -NH- group, a phenomenon known as deprotonation of the membrane [35].

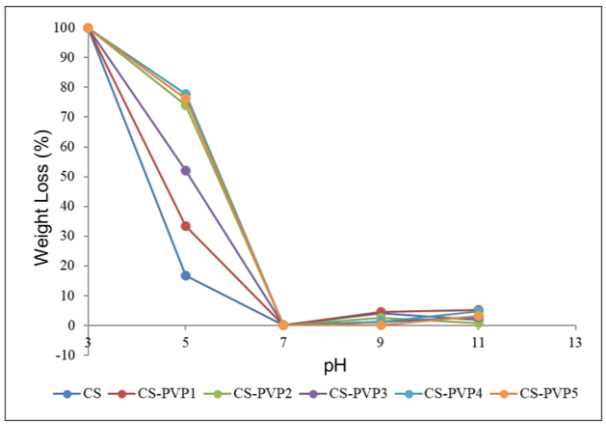

Figure 3. Graph of membrane weight reduction in the pH resistance test

3.2.2. Membrane Biodegradation

The biodegradation test employed the soil burial method, entailing the burial of the membrane in the soil. The membrane's resistance to biodegradation is a crucial parameter related to its capacity to decompose in soil, classifying it as environmentally friendly. In this study, the decomposition process unfolded under aerobic conditions with the participation of soil microorganisms. The membranes were uniformly buried to the same depth and left undisturbed for 15 weeks. Weekly, the membranes were unearthed, cleaned, and weighed, and the decomposition process values are depicted in Figure 4. The results indicate that microorganisms in the soil readily decomposed the membrane. Within 15 weeks, nearly the entire membrane had been completely broken down by these microorganisms. Notably, CS membranes exhibited the highest resistance to microbial degradation compared to other membrane types.

The positive charge of CS, stemming from the protonation of its amine group in an acidic medium, plays a significant role in enhancing its degradability resistance to microbes. Since soil pH is generally acidic, it favors CS protonation, resulting in a positively charged state. This charge augmentation boosts the antimicrobial activity of the membrane, subsequently reducing membrane degradation. In the CS-PVP membrane, the positive charge of CS diminishes due to its interaction with PVP. Consequently, the antimicrobial efficacy of the CS-PVP membrane decreases, leading to increased membrane degradation.

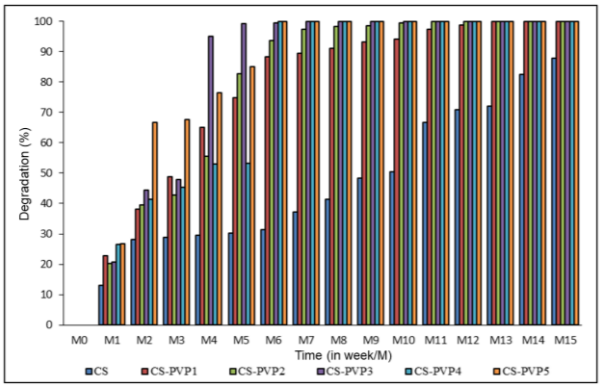

Figure 4. Graph of membrane degradation rate

3.3. Membrane Transport Capability

In this investigation, the transport process endured for 6 hours with samples collected at hourly intervals. The creatinine transport outcomes are depicted in Figure 5.

Creatinine clearance exhibited an increase on the CS membrane modified with PVP. Specifically, the creatinine clearance values for the CS membrane, CS-PVP1, CS- PVP2, CS-PVP3, CS-PVP4, and CS-PVP5 are 0.30, 0.36, 0.37, 0.39, 0.42, and 0.46 mg/dL, respectively. This suggests that modifying the CS membrane with PVP enhances its capability in the creatinine transport process.

The synergy between CS and PVP K-30 contributes to an elevation in the percentage of transported creatinine across the membrane. Creatinine, being a neutral compound, forms hydrogen bonds, particularly in the presence of electronegative compounds. The pyrrolidone ring in PVP incorporates a proton that interacts with the carbonyl moiety, while CS presents carbonyl and amino groups as side groups, fostering hydrogen bonding interactions between these chemical moieties [36]. The amino and hydroxyl groups in CS further engage in hydrogen bonding with the amino groups in creatinine, aligning with the heightened creatinine transport capability of the membrane.

The introduction of PVP K-30 contributes to increased membrane porosity, thereby enhancing the creatinine transport ability. This heightened porosity results from adding additives at low concentrations, enabling complete diffusion and the formation of larger pores [37]. Membranes with increased porosity offer advantages in permeation flux, positively influencing membrane performance. Furthermore, the incorporation of PVP K-30 augments the membrane's hydrophilic properties. The addition of PVP K-30 to CS membranes increases hydrophilicity by leveraging the N-H hydrophilic groups' effect, fostering greater interaction between the membrane and water. Hydrophilic additives tend to migrate to the water interface during the phase inversion process, thereby augmenting the density of hydrophilic hydroxyl groups on the membrane surface and increasing hydrophilicity, subsequently elevating permeation flux [38].

The membrane reuse test, conducted for three uses, as illustrated in Figure 6, reveals a decrease in creatinine clearance values with repeated membrane use. The creatinine clearance values did not significantly decline despite this decrease, indicating commendable stability in the membrane's reactive side. Notably, the CS membrane experienced a 26.67% reduction in clearance performance on the third use, indicating relatively lower durability than other membranes. The addition of PVP to CS enhances the mechanical properties of the membrane, fortifying it and extending its durability.

A distinct outcome emerged in the vitamin B12 transport test, as depicted by the transport results in Table 3. Notably, there was a consistent reduction in feed concentration at each transport time interval, accompanied by an absence of any discernible increase in acceptor concentration. This observation indicates that vitamin B12 molecules are not effectively transported through the membrane. Instead, these molecules are solely retained on the membrane's surface and do not permeate its pores. This phenomenon is attributed to the molecular size of vitamin B12, which is classified as a medium-weight species with a molecular weight of 1355 g/mol, rendering it incapable of passing through the membrane.

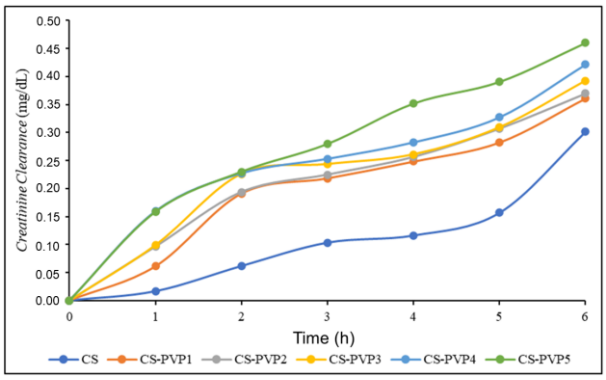

Figure 5. Graph of creatinine clearance

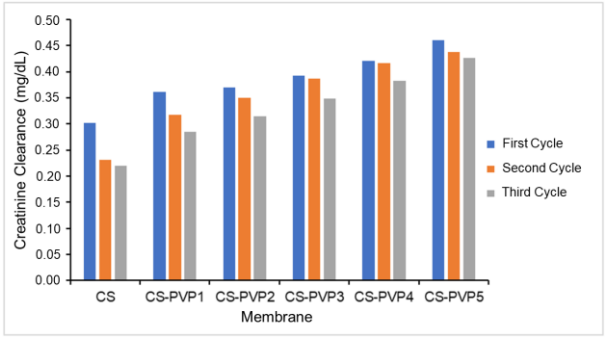

Figure 6. Reusability of membranes in terms of creatinine clearance

Table 3. Results of vitamin B12 transport on the CS-PVP5 membrane

Time (h)	Concentration of vitamin B12 (mg/dL)	
	Feed	Acceptor
0	1.50	0.00
1	1.49	0.00
2	1.47	0.00
3	1.43	0.00
4	1.42	0.00
5	1.33	0.00
6	1.31	0.00

4. Conclusion

The modification of the CS membrane through the incorporation of PVP K-30 has been successfully executed. FTIR analysis substantiated the occurrence of hydrogen bond interactions between CS and PVP K-30. The resultant CS-PVP K-30 membrane exhibits favorable physicochemical attributes. The introduction of PVP contributes to heightened porosity, hydrophilicity, water absorption, and the degree of membrane swelling. Additionally, the membrane's stability against pH variations and biodegradation is enhanced by incorporating PVP. This augmentation is accompanied by improved membrane creatinine transport capability, with the CS-PVP5 membrane demonstrating the most notable transport proficiency.

Acknowledgment

We are grateful for the great support provided by the staff of the analytical chemistry laboratory, FSM, Dipnegoro University, whose unwavering commitment to our research has played an important role in advancing scientific knowledge and encouraging innovation in our field.

References

[1] Retno Ariadi Lusiana, Ginanjar Argo Pambudi, Fitra Nilla Sari, Didik Setiyo Widodo, Khabibi Khabibi, Sri Isdadiyanto, Grafting of Heparin on Blend Membrane of Citric Acid Cross-linked Chitosan/Polyethylene Glycol-Poly Vinyl Alcohol (PVA-PEG), *Indonesian Journal of Chemistry*, 19, 1, (2019), 151-159 https://doi.org/10.22146/ijc.30861

[2] Noresah Said, Woei Jye Lau, Yeek-Chia Ho, Soo Kun Lim, Muhammad Nidzhom Zainol Abidin, Ahmad Fauzi Ismail, A Review of Commercial Developments and Recent Laboratory Research of Dialyzers and Membranes for Hemodialysis Application, *Membranes*, 11, 10, (2021), 767 https://doi.org/10.3390/membranes11100767

[3] Paul L. Kimmel, Depression in patients with chronic renal disease: What we know and what we need to know, *Journal of Psychosomatic Research*, 53, 4, (2002), 951-956 https://doi.org/10.1016/S0022-3999(02)00310-0

[4] Xufeng Yu, Lingdi Shen, Yadong Zhu, Xiong Li, Yin Yang, Xuefen Wang, Meifang Zhu, Benjamin S. Hsiao, High performance thin-film nanofibrous composite hemodialysis membranes with efficient middle-molecule uremic toxin removal, *Journal of Membrane Science*, 523, (2017), 173-184 https://doi.org/10.1016/j.memsci.2016.09.057

[5] Arash Mollahosseini, Amira Abdelrasoul, Novel insights in hemodialysis: Most recent theories on membrane hemocompatibility improvement, *Biomedical Engineering Advances*, 3, (2022), 100034 https://doi.org/10.1016/j.bea.2022.100034

[6] Shamo Zokhrab Tapdigov, The bonding nature of the chemical interaction between trypsin and chitosan based carriers in immobilization process depend on entrapped method: A review, *International Journal of Biological Macromolecules*, 183, (2021), 1676-1696 https://doi.org/10.1016/j.ijbiomac.2021.05.059

[7] S. Islam, M. A. Rahman Bhuiyan, M. N. Islam, Chitin and Chitosan: Structure, Properties and Applications in Biomedical Engineering, *Journal of Polymers and the Environment*, 25, (2017), 854-866 https://doi.org/10.1007/s10924-016-0865-5

[8] O. S. Serbanescu, S. I. Voicu, V. K. Thakur, Polysulfone functionalized membranes: Properties and challenges, *Materials Today Chemistry*, 17, (2020), 100302 https://doi.org/10.1016/j.mtchem.2020.100302

[9] Meng Zhang, Guohui Wang, Dong Wang, Yuqi Zheng, Yanxin Li, Wenqiao Meng, Xin Zhang, Feifan Du, Shaoxiang Lee, Ag@MOF-loaded chitosan nanoparticle and polyvinyl alcohol/sodium alginate/chitosan bilayer dressing for wound healing applications, *International Journal of Biological Macromolecules*, 175, (2021), 481-494 https://doi.org/10.1016/j.ijbiomac.2021.02.045

[10] Shijie Kou, Linda M. Peters, Michael R. Mucalo, Chitosan: A review of sources and preparation methods, *International Journal of Biological Macromolecules*, 169, (2021), 85-94 https://doi.org/10.1016/j.ijbiomac.2020.12.005

[11] Saiful, Lidiya Mardiyana, Rahmi, Khairi Suhud, Yanuardi Raharjo, Chitosan-starch cross-linked citric acid as adsorptive hemodialysis membrane, *Materials Today: Proceedings*, 65, (2022), 2986-2991 https://doi.org/10.1016/j.matpr.2022.03.575

[12] R. Poonguzhali, S. Khaleel Basha, V. Sugantha Kumari, Fabrication of asymmetric nanostarch reinforced Chitosan/PVP membrane and its evaluation as an antibacterial patch for in vivo wound healing application, *International Journal of Biological Macromolecules*, 114, (2018), 204-213 https://doi.org/10.1016/j.ijbiomac.2018.03.092

[13] Nasrul Arahman, Sri Mulyati, Afrillia Fahrina, Syawaliah Muchtar, Mukramah Yusuf, Ryosuke Takagi, Hideto Matsuyama, Nik Abdul Hadi Nordin, Muhammad Roil Bilad, Improving Water Permeability of Hydrophilic PVDF Membrane Prepared via Blending with Organic and Inorganic Additives for Humic Acid Separation, *Molecules*, 24, 22, (2019), 4099 https://doi.org/10.3390/molecules24224099

[14] Muhammad Irfan, Masooma Irfan, Syed Mazhar Shah, Nadeem Baig, Tawfik A. Saleh, Mahmood Ahmed, Gul Naz, Naeem Akhtar, Nawshad Muhammad, Ani Idris, Hemodialysis performance and anticoagulant activities of PVP-k25 and carboxylic-multiwall nanotube composite blended Polyethersulfone membrane, *Materials Science and Engineering: C*, 103, (2019), 109769 https://doi.org/10.1016/j.msec.2019.109769

[15] K. Lewandowska, Surface properties of chitosan composites with poly(N-vinylpyrrolidone) and montmorillonite, *Polymer Science, Series A*, 59, (2017), 215-222 https://doi.org/10.1134/S0965545X17020043

[16] R. Poonguzhali, S. Khaleel Basha, V. Sugantha Kumari, Synthesis and characterization of chitosan/poly (vinylpyrrolidone) biocomposite for biomedical application, *Polymer Bulletin*, 74, (2017), 2185-2201 https://doi.org/10.1007/s00289-016-1831-z

[17] R. H. Sizílio, J. G. Galvão, G. G. G. Trindade, L. T. S. Pina, L. N. Andrade, J. K. M. C. Gonsalves, A. A. M. Lira, M. V. Chaud, T. F. R. Alves, M. L. P. M. Arguelho,

R. S. Nunes, Chitosan/pvp-based mucoadhesive membranes as a promising delivery system of betamethasone-17-valerate for aphthous stomatitis, *Carbohydrate Polymers*, 190, (2018), 339-345 https://doi.org/10.1016/j.carbpol.2018.02.079

[18] Hossein Rahmani, Seyed Heydar Mahmoudi Najafi, Alireza Ashori, Marzieh Arab Fashapoyeh, Farzaneh Aziz Mohseni, Sara Torkaman, Preparation of chitosan-based composites with urethane cross linkage and evaluation of their properties for using as wound healing dressing, *Carbohydrate Polymers*, 230, (2020), 115606 https://doi.org/10.1016/j.carbpol.2019.115606

[19] Qiu Gen Zhang, Wen Wei Hu, Ai Mei Zhu, Qing Lin Liu, UV-crosslinked chitosan/polyvinylpyrrolidone blended membranes for pervaporation, *RSC Advances*, 3, (2013), 1855-1861 https://doi.org/10.1039/C2RA21827E

[20] Hasan Muhtar, Adi Darmawan, Fabrication of negatively charged nanofiltration membrane of modified polystyrene intercalated graphene oxide for pervaporation desalination, *Chemical Engineering Journal*, 475, (2023), 146095 https://doi.org/10.1016/j.cej.2023.146095

[21] Retno Ariadi Lusiana, Vivi Dia Ahmad Sangkota, Sri Juari Santosa, Chitosan succinate/PVA-PEG Membrane: Preparation, Characterization and Permeation Ability Test on Creatinine, *Jurnal Kimia Sains dan Aplikasi*, 21, 2, (2018), 80-84 https://doi.org/10.14710/jksa.21.2.80-84

[22] Retno Ariadi Lusiana, Dian Tri Pratama, Hasan Muhtar, Facile modification of polyvinylidene fluoride membrane for enhancing dialysis performance: sulfonation, adding polyethylene glycol and tuning coagulation bath temperature, *Journal of Macromolecular Science, Part A*, (2023), 1-12 https://doi.org/10.1080/10601325.2023.2287044

[23] Shih-Hsien Wang, Peter R. Griffiths, Resolution enhancement of diffuse reflectance i.r. spectra of coals by Fourier self-deconvolution: 1. C-H stretching and bending modes, *Fuel*, 64, 2, (1985), 229-236 https://doi.org/10.1016/0016-2361(85)90223-6

[24] Mohammed S. Al Mogbel, Mohamed T. Elabbasy, Rasha S. Mohamed, A. E. Ghoniem, M. F. H. Abd El-Kader, A. A. Menazea, Improvement in antibacterial activity of Poly Vinyl Pyrrolidone/Chitosan incorporated by graphene oxide NPs via laser ablation, *Journal of Polymer Research*, 28, (2021), 474 https://doi.org/10.1007/s10965-021-02838-x

[25] Qianzhu Li, Dongzhi Yang, Guiping Ma, Qiang Xu, Xiangmei Chen, Fengmin Lu, Jun Nie, Synthesis and characterization of chitosan-based hydrogels, *International Journal of Biological Macromolecules*, 44, 2, (2009), 121-127 https://doi.org/10.1016/j.ijbiomac.2008.11.001

[26] Saima Sultana, Nafees Ahmad, Syed M. Faisal, M. Owais, Suhail Sabir, Synthesis, characterisation and potential applications of polyaniline/chitosan-Ag-nano-biocomposite, *IET Nanobiotechnology*, 11, 7, (2017), 835-842 https://doi.org/10.1049/iet-nbt.2016.0215

[27] Mohammed Eddya, Bouazza Tbib, Khalil El-Hami, A comparison of chitosan properties after extraction from shrimp shells by diluted and concentrated acids, *Heliyon*, 6, 2, (2020), E03486 https://doi.org/10.1016/j.heliyon.2020.e03486

[28] Ritesh Kumar, Indrani Mishra, Gulshan Kumar, Synthesis and Evaluation of Mechanical Property of Chitosan/PVP Blend Through Nanoindentation-A Nanoscale Study, *Journal of Polymers and the Environment*, 29, (2021), 3770-3778 https://doi.org/10.1007/s10924-021-02143-0

[29] Adi Darmawan, Anjalya Figo Nur Sabarina, Damar Nurwahyu Bima, Hasan Muhtar, Christina Wahyu Kartikowati, Teguh Endah Saraswati, New design of graphene oxide on macroporous nylon assisted polyvinyl alcohol with Zn (II) cross-linker for pervaporation desalination, *Chemical Engineering Research and Design*, 195, (2023), 54-64 https://doi.org/10.1016/j.cherd.2023.05.029

[30] B. Chakrabarty, A. K. Ghoshal, M. K. Purkait, Preparation, characterization and performance studies of polysulfone membranes using PVP as an additive, *Journal of Membrane Science*, 315, 1, (2008), 36-47 https://doi.org/10.1016/j.memsci.2008.02.027

[31] M. O. Mavukkandy, M. R. Bilad, J. Kujawa, S. Al-Gharabli, H. A. Arafat, On the effect of fumed silica particles on the structure, properties and application of PVDF membranes, *Separation and Purification Technology*, 187, (2017), 365-373 https://doi.org/10.1016/j.seppur.2017.06.077

[32] David Aili, Mikkel Rykær Kraglund, Joe Tavacoli, Christodoulos Chatzichristodoulou, Jens Oluf Jensen, Polysulfone-polyvinylpyrrolidone blend membranes as electrolytes in alkaline water electrolysis, *Journal of Membrane Science*, 598, (2020), 117674 https://doi.org/10.1016/j.memsci.2019.117674

[33] Xiaorui Ren, Huanhuan Li, Ke Liu, Hongyi Lu, Jingshuai Yang, Ronghuan He, Preparation and Investigation of Reinforced PVP Blend Membranes for High Temperature Polymer Electrolyte Membranes, *Fibers and Polymers*, 19, 12, (2018), 2449-2457 https://doi.org/10.1007/s12221-018-8361-2

[34] Caiqin Qin, Huirong Li, Qi Xiao, Yi Liu, Juncheng Zhu, Yumin Du, Water-solubility of chitosan and its antimicrobial activity, *Carbohydrate Polymers*, 63, 3, (2006), 367-374 https://doi.org/10.1016/j.carbpol.2005.09.023

[35] Yang Liu, Chuang Lang, Yaping Ding, Siyu Sun, Guangwei Sun, Chitosan with enhanced deprotonation for accelerated thermosensitive gelation with β -glycerophosphate, *European Polymer Journal*, 196, (2023), 112229 https://doi.org/10.1016/j.eurpolymj.2023.112229

[36] Jen-Taut Yeh, Chin-Lai Chen, K. S. Huang, Y. H. Nien, J. L. Chen, P. Z. Huang, Synthesis, characterization, and application of PVP/chitosan blended polymers, *Journal of Applied Polymer Science*, 101, 2, (2006), 885-891 https://doi.org/10.1002/app.23517

[37] Cristiana M. P. Yoshida, Enio Nazaré Oliveira Junior, Telma Teixeira Franco, Chitosan tailor-made films: the effects of additives on barrier and mechanical properties, *Packaging Technology and Science*, 22, 3, (2009), 161-170 https://doi.org/10.1002/pts.839

[38] Mohtada Sadrzadeh, Subir Bhattacharjee, Rational design of phase inversion membranes by tailoring thermodynamics and kinetics of casting solution using polymer additives, *Journal of Membrane Science*, 441, (2013), 31-44 https://doi.org/10.1016/j.memsci.2013.04.009